Progress In Electromagnetics Research B, Vol. 24, 317–331, 2010

DESIGN AND ANALYSIS OF MICROSTRIP REFLECTARRAY ANTENNA WITH MINKOWSKI SHAPE RADIATING ELEMENT

F. Zubir, M. K. A. Rahim, O. Ayop, A. Wahid and H. A. Majid

Faculty of Electrical Engineering
Department of Radio Communication Engineering
Universiti Teknologi Malaysia
Skudai, Johor 81310, Malaysia

Abstract—This paper describes the design and analysis of a Microstrip Reflectarray Antenna (MRA) with Minkowski shape radiating element at frequency of 11 GHz. This structure has been analyzed and compared with the traditional reflectarray element (square element patch). It is found that this antenna array has lower sidelobe level (SLL) characteristic which is down to −25 dB. This MRA has maximum realized gain of 29.6 dB with half-power beamwidth (HPBW) of 3.7°. The validation for the proposed MRA is done by comparing the simulated and measured E-plane radiation pattern. A very good agreement is found from the comparison between simulation and measurement.

1. INTRODUCTION

The need for high-gain antenna is essential and unavoidable since it plays a vital role in a long distance wireless communications. Conventionally, the application for most radar and long haul communication that requires such a high-gain antenna has relied on parabolic reflectors or arrays [1]. In certain cases, the parabolic reflector is difficult to manufacture due to its curved surface especially at higher microwave frequencies for satellite applications [2]. In addition, active or passive phased arrays may contribute to the complexity and losses on the antenna itself because of the existing of the power division transmission lines and any other electronic devices

Received 12 July 2010, Accepted 10 August 2010, Scheduled 18 August 2010
Corresponding author: F. Zubir (farid@fke.utm.my).

being attached to it [3]. As a result, a third type of antenna which is called "microstrip reflectarray" has been developed gradually to make less severe problem associated with either parabolic reflector or the conventional array, thus providing a higher efficiency.

Phase compensation is essential in designing reflectarray. It is very important for reflectarrays to have behavior just like a conventional parabolic type of reflector which will focus and reflect the particular rays towards intended position or receiver (horn antenna). Otherwise, reflectarray will have the same behavior as a normal metal plate or ground plane where it will scatter the rays away from the receiver. Therefore, all elements on the reflectarray plane are required to be specifically designed with the appropriate phase because the incident wave will propagate and presents a different phase from one element to another.

There are a few kinds of phase compensation methods available for the fixed-beam reflectarray such as using open-circuited stubs [4], variable patch size [5], slot-loaded ground plane [6], slot-loaded patch [7] and the usage of electronic components [8]. Stubs produce some dissipative losses as well as spurious radiation when it is being bent. Besides, an extra space or room should be reserved for the open-circuited stub on the reflectarray layout. The method as suggested in [6] may produce a backward radiation, which is the reason why [7] had been proposed to reduce as well as overcome those backward radiations. However, method in [7] has limited phase variation because of due to its patch size. The integration of electronic components in one patch as proposed in method [8] may contribute many losses and complexity so bad that it is very hard to analyze especially when applied to arrays at millimeter-wave frequency [9]. In this work, a method of patch with variable size is used because of the benefits stated in [10], and it is expected to be better than other methods.

All the phase compensation methods that have been mentioned above were using square or rectangular patch as their array elements which are assumed as not good enough to be employed in the reflectarray design. The sidelobe level (SLL), realized gain (dB) and phase-shift (°) are among the concerns in the design considerations. Therefore, in this work, avoiding complexity and losses at the millimeter-wave frequency as well as other consequences of the conventional shape radiating element is the rationale for developing a novel configuration of the passive reflectarray unit cell which is using first iteration of fractal's shape like Minkowski as a radiating element in the MRA design. Unlike in [11], the employment of the fractal geometry (Minkowski) in a normal antenna design (direct feed by coaxial probe) was purposely to achieve multiband frequency

operation and compactness. On the other hand, compared with the conventional structure, which are using basic square or rectangular shape as array elements [12–14], this reflectarray unit cell is able to provide low insertion loss and acceptable phase range (phase-shift). With those advantages, a moderate aperture size of single layer passive microstrip reflectarray with practically used f/D ratio [15] is developed. This fixed beam microstrip reflectarray is capable of providing better realized gain (dB) with lower SLL at 11 GHz when compared with the conventional ones.

2. UNIT CELL DESIGN

The theoretical analysis is implemented using available full-wave simulation tool Computer Simulation Technology Microwave Studio (CST MWS). Basic building block for a single layer unit cell of reflectarray is designed at X-band frequency of 11 GHz. Minkowski, and basic square element geometry is proposed to be a resonant element shape for a periodic reflectarray structure separately. Fig. 1 shows the dimensions for both Minkowski and square element at the same resonant frequency of 11 GHz where the radiating patch with patch width $m = 5.41$ mm and $v = 6.06$ mm respectively is printed on the substrate material RF-35. The geometry of Minkowski is created using iteration factor as depicted in [16]. Generally, the value of s is smaller than $m/3$. In this work, a value of iteration factor, $\eta = 0.75$, is exploited in order to design the geometry of Minkowski. For the phase compensation, only patch dimension, m, is varied in percentage while the other parameters remain fixed.

$$\eta = \frac{s}{m/3}; \quad 0 < \eta < 1 \tag{1}$$

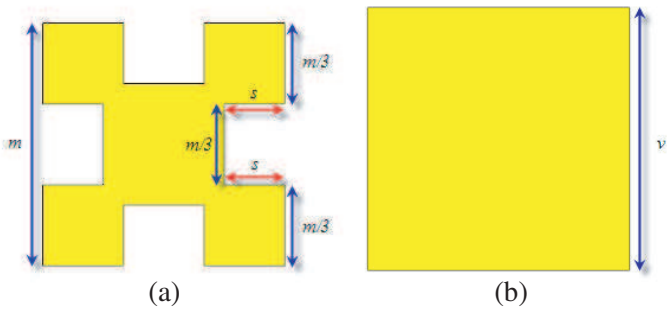

Figure 1. The dimensions of element geometry. (a) Minkowski. (b) Square.

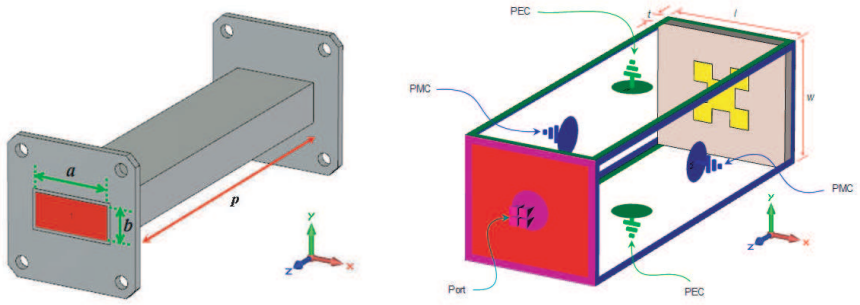

Figure 2. (a) Illustration of existing standard X-band waveguide. (b) Microstrip reflectarray unit cell in the TEM-mode waveguide.

The periodicity of the unit cell reflectarray is based on the existing standard waveguide dimension. Fig. 2(a) shows the geometry of rectangular waveguide (X-band) that has been used as a reference in term of its dimension to design a unit cell for reflectarray, and Fig. 2(b) shows a boundary condition in the simulation setup for TEM-mode propagation (Infinite Array Approach). Meanwhile, the rational of choosing the waveguide dimension in determining the size of reflectarray unit cell is for the ease of measuring the reflection coefficient. Substrate selection including material such as relative permittivity (ε_r), tangential loss ($\tan\delta$), thickness (t) and element periodicity ($l \times w$) has been taken into account. Each element is designed to be printed on a substrate with thickness ($t = 1.524\,\text{mm}$), tangential loss ($\tan\delta = 0.0018$), and relative permittivity ($\varepsilon_r = 3.54$). Since the dimension of standard waveguide is $a = 22.86\,\text{mm}$, $b = 10.16\,\text{mm}$ and $p = 120\,\text{mm}$, a suitable periodicity of the unit cell reflectarray is $l = 11.43\,\text{mm}$ and $w = 10.16\,\text{mm}$, with a copper thickness of $0.035\,\text{mm}$.

In the simulation, there is only one unit cell being excited using TEM-mode. In this mode, a unit cell is actually illuminated by a linearly polarized plane wave with a normal incidence angle. In the real world, there is no such way to excite the corresponding unit cell using TEM-mode propagation. Therefore, a real metallic waveguide is needed in order to measure the phase variation of the proposed unit cell configuration. In this case, a unit cell will be excited by a coaxial probe of the waveguide adapter which using TE_{10} mode. Even though they are two different modes of excitation, it would not affect much on the overall performance of the unit cell itself because it just has the correlation with the angle of incidence. Angle of incidence actually does not strongly influence the resonant frequency since the elements

are arranged in a close-packed [17–18].

3. PHASE-SHIFT OF A UNIT CELL

In this work, a coordinate system has been used to determine the progressive phase distribution on the microstrip reflectarray surface with a centered focal point that will produce a pencil beam in a direction of normal to the surface. Having said that, the equations expressed in (2) until (5) as below have been used to obtain the required phase-shift at each element [9, 13]. A diagram in Fig. 3 representing a reflectarray layout with a feed horn at its focal point will be helpful to understand the equations given below:

$$d_i = \left[\sqrt{[(i) \times x]^2 + [(j) \times y]^2}\right] \times 10^{-3} \tag{2}$$

$$f = D \times h \tag{3}$$

$$l = \sqrt{f^2 + d^2} \tag{4}$$

$$\phi_r = \frac{2\pi}{\lambda} \times (l - f) \tag{5}$$

where:

i = Coordinate at x-axis.

j = Coordinate at y-axis.

x = Length of unit cell.

y = Width of unit cell.

f = Prime focus distance.

D = Largest dimension of the microstrip reflectarray.

h = Prime focus to large dimension ratio (f/D).

l = Path length from the feed horn.

d = On-board distance from reference focus point to element.

ϕ_r = Required phase-shift.

λ = Wavelength of the operating frequency.

After obtaining the required phase-shift at the respective unit cells, a contour phase distribution on a rectangular reflectarray of 37×29 elements ($422.91 \times 294.64\,\text{mm}^2$) with $f/D = 0.8$ at 11 GHz is plotted as shown in Fig. 4(a). Meanwhile, the 3D phase distribution, as shown in Fig. 4(b), illustrates the equivalent conventional parabolic type of reflector on the reflectarray plane for the proposed MRA.

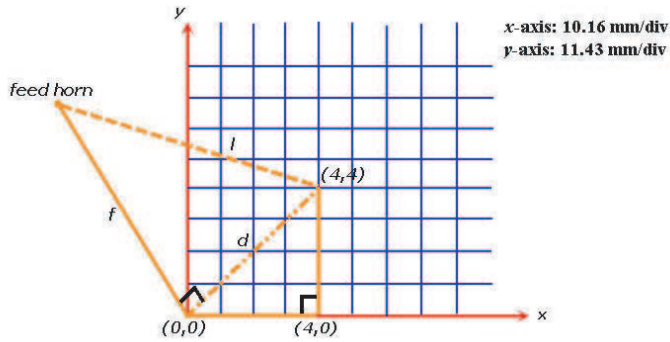

Figure 3. A diagram of coordinate system in determining phase-shift of each reflectarray unit cell.

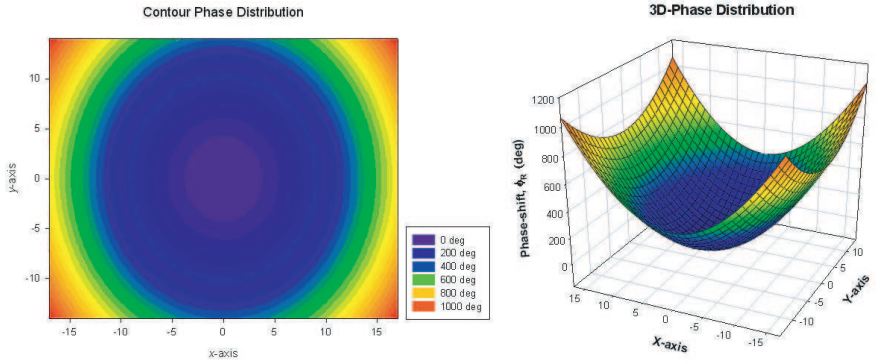

(a) (b)

Figure 4. (a) Contour phase distribution on a rectangular reflectarray at 11 GHz. (b) Equivalent parabolic reflector on the reflectarray plane.

4. SIMULATION RESULT

4.1. Reflectarray Unit Cell

Parameter sweep has been conducted on a single layer of reflectarray unit cell, and it has been specified to obtain a resonance frequency of 11 GHz. The geometry of resonant element patch is swept with a patch variation, $n = \pm 2$, from their resonant size which is $n = 0$. For example, $n = +2$ means the patch is 20% larger than its resonant size and vice versa. Fig. 5 shows a simulated reflection magnitude and phase-shift of the reflectarray unit cell at 11 GHz with

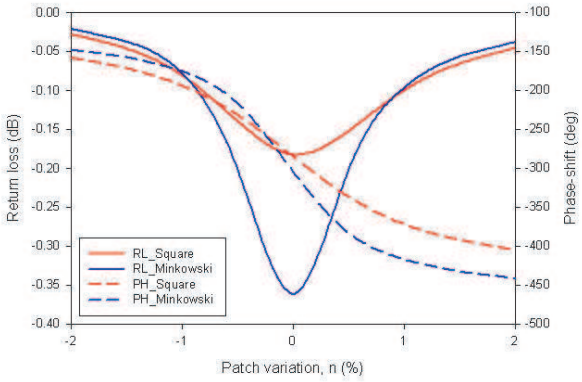

Figure 5. Reflection coefficient responses at $f = 11\,\text{GHz}$.

Minkowski and Square shape element patch respectively. As can be seen, both reflectarray unit cells configurations exhibit at desired reflection magnitude which does not even reach 1 dB. Moreover, it can be observed from the figure below where the maximum achievable reflection phase range for the unit cell with Minkowski element (300°) is wider than unit cell with square element (250°).

In terms of reflection, even though Minkowski patch ($-0.35\,\text{dB}$ = 92% reflection) has more losses compared to square patch ($-0.17\,\text{dB}$ = 96% reflection), by calculation both shapes still have about more than 90% reflection at resonant frequency (11 GHz), which comply with our design consideration (we are designing a *reflector*). However, this characteristic is not our main concern but still included in the considerations. The concerns are more towards the gain and SLL that could be realized by the reflectarray using Minkowski and square element separately. From the simulation, we found that reflectarray which using Minkowski shape as array elements is managed to perform well compared to the other structure. Minkowski element is capable of providing wider phase range (300°) compared to square element (250°). Actually, at the first place, when we look at the patch distributions over the reflectarray surface (see Fig. 6), we can say that the structure with Minkowski elements will perform better because the structure has more patches compared to square. Having said that, even though the difference in the phase variation is only 50°, it can still affect much in the overall performance of the reflectarray as this 50° will cause the structure to have many regions with no radiating element at all. Consequently, due to this region, rise of the grating lobes and phase error will occur. As a result, it will reduce the efficiency, gain and HPBW simultaneously.

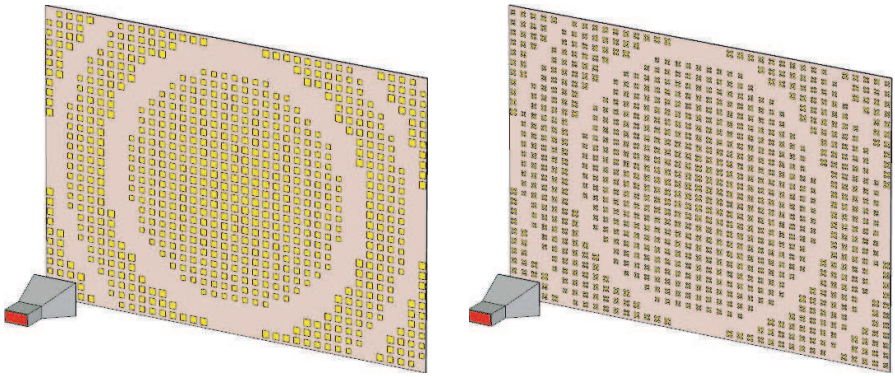

(a) (b)

Figure 6. Simulated MRA structures. (a) MRA with square elements. (b) MRA with Minkowski elements.

4.2. Microstrip Reflectarray Antenna (MRA)

Based on the analysis of the reflectarray unit cell (phase-shift graph), patches with the appropriate phase delay could be distributed over the reflectarray plane. In order to investigate the performance of the proposed MRA structures, two prototypes of MRA have been designed and simulated using CST MWS and thus, it will be compared to each other. Fig. 6 illustrates the patch distributions over the reflectarray surface with a feed horn takes place at a focal point respectively. Obviously, it can be seen that reflectarray with Minkowski radiating elements is the structure most occupied by the radiating elements compared to the structure with square radiating elements. Actually, typical X-band rectangular pyramidal horn antenna ($42 \times 31\,\text{mm}^2$) that has gain around 12–13 dB has been used to be incorporated with the proposed microstrip reflectarray.

The simulation of both MRAs is to investigate the performances of both proposed structures. The simulation results show the efficiency, realized gain, half-power beamwidth (HPBW) and SLL. Fig. 7(a) and Fig. 7(b) show the simulated 3-D farfield radiation pattern at 11 GHz for the corresponding MRA designs, respectively. Fig. 7(a) shows that the realized gain of the MRA with square shape is 27.41 dB with a total efficiency -0.1941 dB or 95.6 %, while Fig. 7(b) indicates the realized gain of the MRA with the fractal shape (Minkowski) is 29.62 dB with a total efficiency of -0.3947 dB or 91.3%. Meaning, there is a gain increment around 14.4 dB and 16.6 dB for Microstrip Reflectarray Antenna with square and Minkowski elements respectively.

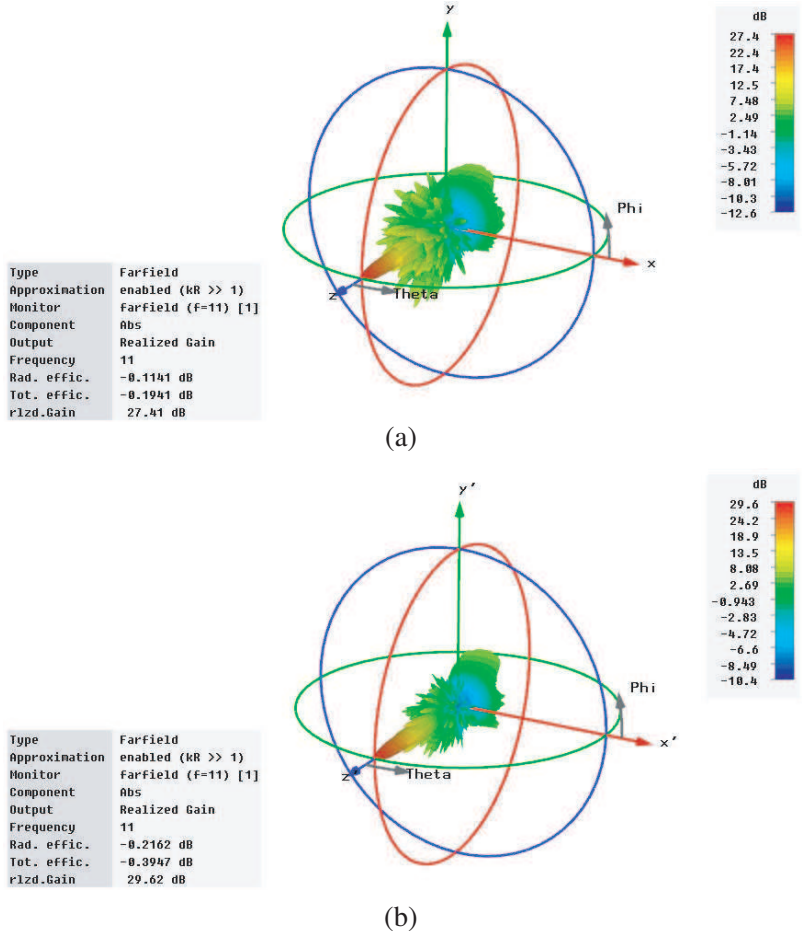

Figure 7. 3-D radiation pattern. (a) MRA with square elements. (b) MRA with Minkowski elements.

Figure 8 shows the Cartesian plot of the radiation patterns at 11 GHz in E-plane. Observation from the Cartesian plot where the SLL for both MRAs (Minkowski and square) obviously can be predicted, which are around -25 dB and -19 dB, respectively. Besides, the HPBW could be obtained from the same graph as well which is about 3.7° and 3.6° for Minkowski and square reflectarray, respectively.

Overall, from the simulation results obtained, it is found that MRA with Minkowski radiating elements is able to perform better than conventional MRA with square shape of radiating elements. As expected, the MRA with Minkowski shape of radiating elements may

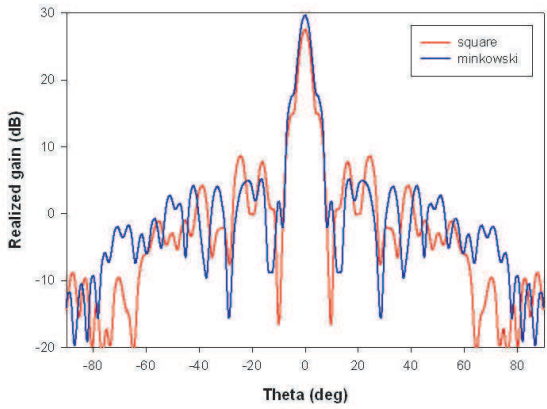

Figure 8. Radiation pattern in Cartesian plot.

provide higher realized gain, good total efficiency as well as very low SLL due to its wider reflection phase range (300°) compared to the MRA with square elements (250°).

The wider reflection phase means higher number of radiating elements occupying the reflectarray surface. When lower number of radiating elements takes place on the reflectarray surface, there will be many spaces with no radiating element at all. As a consequence, the particular spaces or positions which do not occupy any radiating element with the appropriate phase shift will contribute to phase error. The increase of phase error will significantly increase the side-lobe level and thus reduce the gain for the MRA itself. The simulation results for both MRA designs are summarized in Table 1:

Table 1. Summarized of the simulation results analysis.

	MRA with Minkowski radiating elements	**MRA with square radiating elements**
Operating frequency	11 GHz	11 GHz
Realized gain	29.6 dB	27.4 dB
Side-lobe level (SLL)	−25 dB	−19 dB
HPBW	3.7°	3.6°
Total efficiency	91.3%	95.6%

5. EXPERIMENTAL VALIDATION

5.1. Unit Cell with Minkowski Element

A desired configuration of reflectarray unit cell (Minkowski element) has been chosen to undergo the validation procedure. Five configurations of reflectarray unit cell with different patch variations ($n = -2, -1, 0, 1, 2$) have been fabricated to cover the desired frequency range (11 GHz). In this work, the reflection phase variation measurement is done using existing standard X-band rectangular metallic waveguide ($22.86 \times 10.16\,\text{mm}^2$) with $p = 120\,\text{mm}$ which has been excited by a coaxial probe of the waveguide adapter. As usual, a standard coaxial calibration procedure (open, short, load) is conducted before the measurement is being executed.

The experimental result of the corresponding reflectarray unit cell has been compared with the waveguide-based simulation result. The comparison is made based on its variation of the reflection phase. The graphs of reflection phase for both simulated and measured results are plotted according to their patch variation as shown in Fig. 9. As expected, a small phase shift as well as the reflection phase range is observed when compared with the experimental and simulated result. This might be due to the thickness of the glue that has been used to assemble the reflectarray unit cell to a reference plane. Furthermore, probably a shifting in the reflection phase which is around 5° to 20° and the reflection phase range difference ($\sim 3°$) are caused by the misalignment or imperfect cutting-edge of the reflectarray unit cell under test. However, the agreement between simulated and measured reflection phases is considered good enough since its pattern correlates well to each other. Table 2 shows a tabulated data from both simulation and measurement.

Table 2. Tabulated reflection phase variation.

Patch variation, n	Simulated reflection phase	Measured Reflection phase	Difference
−2	6.4797°	−16.5188°	10.0391°
−1	−19.0891°	−39.6383°	20.5492°
0	−178.9874°	−196.3713°	17.3839°
1	−284.6809°	−290.3985°	5.7176°
2	−304.348°	−323.4595°	19.1115°

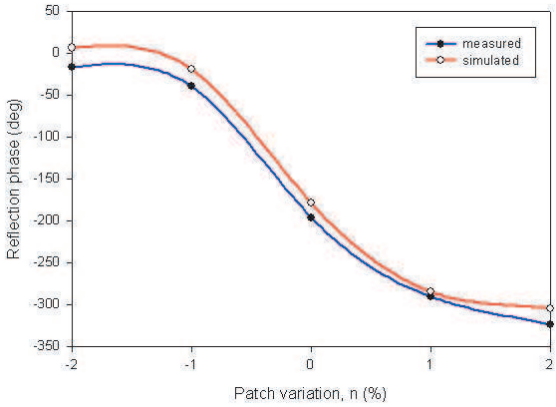

Figure 9. Simulated and measured reflection phase variations.

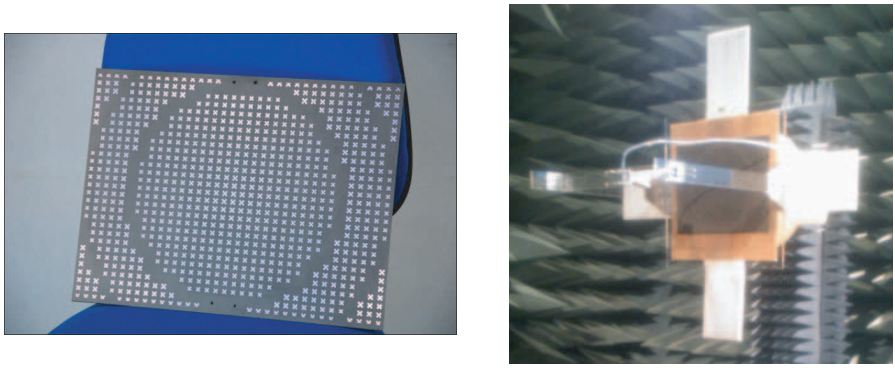

(a) (b)

Figure 10. (a) Fabricated microstrip reflectarray. (b) MRA during the radiation pattern measurement.

5.2. MRA with Minkowski Elements

In practice, the measurement is required to be performed in an appropriate anechoic chamber. A measured far-field radiation pattern for the MRA could be obtained, and it was compared with the simulated radiation pattern provided by the simulation tool, CST MWS software. Fig. 10(a) shows the fabricated microstrip reflectarray after the cleaning process, while Fig. 10(b) shows the prototype of MRA in the anechoic chamber during the measurement of the radiation pattern.

Figure 11(a) shows a measured 3D radiation pattern for the MRA. As can be seen, the main beam of the radiation pattern is directional because the MRA is a high-gain type of antenna. Meanwhile, Fig. 11(b) shows the comparison between simulated and measured radiation patterns for the MRA in Cartesian plot. Both radiation patterns are plotted in the range of $-90°$ to $90°$, and the magnitude of the radiation pattern has been normalized for better viewing and easy to analyze. By referring to Fig. 11(b), the SLL and HPBW for both simulation and measurement could be summarized as in Table 3. Besides, it can be observed that there was a slight difference in terms of their HPBW and SLL, due to the fabrication tolerance and misalignment during measurement setup. However, both results correlate well to each other since the pattern is similar.

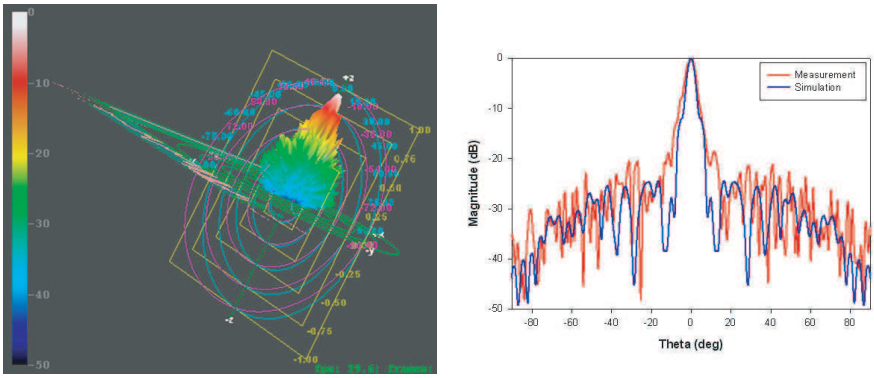

(a) (b)

Figure 11. (a) Measured 3-D radiation pattern. (b) Measured and simulated radiation pattern in Cartesian plot.

Table 3. Summarized of the analysis for both simulated and measured MRA.

	Simulated MRA	**Measured MRA**
Operating frequency	11 GHz	11 GHz
Sidelobe level (SLL)	-25 dB	-21 dB
HPBW	3.7°	3.6°

6. CONCLUSION

This paper presents a design and analysis of microstrip reflectarray antenna with Minkowski shape radiating elements. Compared with conventional MRA structures using basic square shape as array elements, this fixed-beam microstrip reflectarray antenna is capable of providing higher realized gain and lower sidelobe level (SLL). A good agreement was achieved as the validation of the MRA and reflectarray unit cell were successfully done by comparing the results between the simulation and measurement.

ACKNOWLEDGMENT

The authors thank the Ministry of Science Technology and Innovation (MOSTI) for supporting the research work, Research Management Centre (RMC) and Radio Communication Engineering Department (RaCED), Universiti Teknologi Malaysia (UTM) for the support of the research works.

REFERENCES

1. Jasik, H., *Antenna Engineering Handbook*, Chapters 12 and 15, MaGraw-Hill, New York, 1961.
2. Legay, H., et al., "Satellite antennas based on MEMS tuneable reflectarrays," *Proc. Antennas Propagation, EUCAP 2007*, Vol. 1–6, No. 11–16, 2007.
3. Yuan, T., N. Yuan, L.-W. Li, and M.-S. Leong, "Design and analysis of phased antenna array with low sidelobe by fast algorithm," *Progress In Electromagnetics Research*, Vol. 87, 131–147, 2008.
4. Targonski, S. D. and D. M. Pozar, "Analysis and design of a microstrip reflectarray using patches of variable size," *IEEE Symposium on Antennas and Propagation*, Vol. 3, 1820–1823, 1994.
5. Pozar, D. M. and T. A. Metzler, "Analysis of a reflectarray antenna using microstrip patches of variable size," *Electronic letters*, 657–658, April 1993.
6. Chacharmir, M. R., J. Shaker, M. Cuhaci, and A. Sebak, "Reflectarray with variable slots on ground plane," *IEEE Proc. Microwave, Antennas and Propagat.*, Vol. 150, No. 6, 436–439, December 2003.

7. Cadoret, D., A. Laisne, R. Gillard, L. Le Coq, and H. Legay, "A new reflectarray cell using microstrip patches loaded with slots," *Microwave and Optical Technology Letters*, Vol. 41, No. 11, 623–624, May 2005.
8. Tahir, F. A., H. Aubert, and E. Girard, "Equivalent electrical circuit for designing MEMS-controlled reflectarray phase shifters," *Progress In Electromagnetics Research*, Vol. 100, 1–12, 2010.
9. Huang, J. and J. Encinar, *Reflectarray Antennas*, Wiley Interscience, A John Wiley & Sons, Inc., 2008.
10. Pozar, D. M. and T. A. Metzler, "Analysis of a reflectarray antenna using microstrip patches of variable size," *Electronic letters*, 657–658, April 1993.
11. Mahatthanajatuphat, C., S. Saleekaw, and P. Akkaraekthalin, "A rhombic patch monopole antenna with modified minkowskii fractal geometry for UMTS, WLAN, and mobile WIMAX application," *Progress In Electromagnetics Research*, Vol. 89, 57–74, 2009.
12. Javor, R. D., X. D. Wu, and K. Chang, "Design and performance of a microstrip reflectarray antenna," *IEEE Transactions on Antennas and Propagation*, Vol. 43, No. 9, September 1995.
13. Pozar, D. M., S. D. Targonski, and H. D. Syrigos, "Design of millimeter wave microstrip reflectarrays," *IEEE Transactions on Antennas and Propagation*, Vol. 45, No. 2, February 1997.
14. Encinar, J. A. and J. Agustin Zornoza, "Three-layer printed reflectarrays for contoured beam space applications," *IEEE Transactions on Antennas and Propagation*, Vol. 52, No. 5, May 2004.
15. Pozar, D. M., "Bandwidth of reflectarrays," *Electronic Letter*, Vol. 39, No. 21, October 16, 2003.
16. Mahatthanajatuphat, C. and P. Akkaraekthalin, "An NP generator model for Minkowski fractal antenna," *Proceeding of the 3rd ECTI-CON*, Vol. 2, 749–752, 2006.
17. Parker, E. A. and S. M. A. Hamdy, "Rings elements for frequency selective surfaces," *Electronics Letters*, Vol. 17, No. 17, 612–614, 1982.
18. Cahill, R. and E. A. Parker, "Concentric ring and Jerusalem cross arrays as frequency selective surfaces for a 45° incident diplexer," *Electronics Letters*, Vol. 18, No. 8, 313–314, 1982.